Differential effects of Kv7 (M-) channels on synaptic integration in distinct subcellular compartments of rat hippocampal pyramidal neurons

Mala M. Shah[1], Michele Migliore[2] and David A. Brown[3]

[1] *Department of Pharmacology, School of Pharmacy, University of London, London, UK*

[2] *Institute of Biophysics, National Research Council, Palermo, Italy*

[3] *Department of Neuroscience, Physiology and Pharmacology, University College, London, London, UK*

Non-technical summary Ion channels are pores that allow the exchange of molecules across cell membranes. In nerve cells (neurons) of the hippocampus (a brain region involved in learning and memory), the potassium K_V7 channel is present predominantly in the cell body (the soma) and in its axon, a projection from the cell body that produces brief electrical signals known as action potentials. We have previously shown that axonal K_V7 channels control action potential initiation and so regulate cell excitability. However, cells also receive inputs from other cells connected to them, resulting in longer lasting electrical signals known as synaptic potentials. In this study, we show that only somatic K_V7 channels influence synaptic potential shapes and summation, whereas axonal channels increase the ability of synaptic potentials to generate action potentials. Hence, axonal and somatic K_V7 channels differentially contribute to information processing within hippocampal neurons, which may be important for processes such as cognition

Abstract The K_V7/M-current is an important determinant of neuronal excitability and plays a critical role in modulating action potential firing. In this study, using a combination of electrophysiology and computational modelling, we show that these channels selectively influence peri-somatic but not dendritic post-synaptic excitatory synaptic potential (EPSP) integration in CA1 pyramidal cells. K_V7/M-channels are highly concentrated in axons. However, the competing peptide, ankyrin G binding peptide (ABP) that disrupts axonal K_V7/M-channel function, had little effect on somatic EPSP integration, suggesting that this effect was due to local somatic channels only. This interpretation was confirmed using computer simulations. Further, in accordance with the biophysical properties of the K_V7/M-current, the effect of somatic K_V7/M-channels on synaptic potential summation was dependent upon the neuronal membrane potential. Somatic K_V7/M-channels thus affect EPSP–spike coupling by altering EPSP integration. Interestingly, disruption of axonal channels enhanced EPSP–spike coupling by lowering the action potential threshold. Hence, somatic and axonal K_V7/M-channels influence EPSP–spike coupling via different mechanisms. This may be important for their relative contributions to physiological processes such as synaptic plasticity as well as patho-physiological conditions such as epilepsy.

Abbreviations ABP, ankyrin G binding peptide; αEPSP, simulated EPSP waveform

Introduction

K_V7 channels underlie the so-called 'M'-current, a sub-threshold active neuronal K^+ current (Brown & Passmore, 2009). All five known subtypes ($K_V7.1$–7.5) are likely to be expressed in central neurons (Brown & Passmore, 2009; Goldman *et al.* 2009). Although early reports indicated that these neurons may have a somato-dendritic expression pattern (Roche *et al.* 2002; Shah *et al.* 2002), recent reports suggest that these channels are expressed at a higher density in axons (Devaux *et al.* 2004; Chung *et al.* 2006; Pan *et al.* 2006). Here, they play a role in regulating the resting membrane potential and action potential threshold (Shah *et al.* 2008), and thereby influence post-synaptic spike firing. This may be one of the potential mechanisms that enhance neuronal excitability during benign familial neonatal convulsions (BFNC) as mutations in K_V7/M-channels associated with this condition can result in disrupted axonal K_V7 channel function (Chung *et al.* 2006).

In vivo, though, excitatory synaptic potential (EPSP) integration is an important factor in determining action potential generation (Debanne, 2004; Clark & Hausser, 2006). Since K_V7 channels are active at rest (Shah *et al.* 2008), it is possible that they may contribute to synaptic potential integration. Indeed, the summation of a train of EPSPs generated by extracellular stimulation in hippocampal CA1 pyramids is affected by K_V7/M-channel modulation (Hu *et al.* 2007). However, since K_V7/M-channels may also be present pre-synaptically in the hippocampus (Martire *et al.* 2004; Peretz *et al.* 2007), it is not clear whether this effect is pre- or post-synaptic in origin. In this study, we injected EPSP waveforms (αEPSPs) in the soma and dendrites of CA1 pyramids to investigate how EPSP integration is affected in these neuronal sub-cellular compartments. We also used a competing peptide, ankyrin G binding peptide (ABP; Shah *et al.* 2008) to determine if axonal K_V7 channels contribute to somatic EPSP summation. Computer simulations were performed to corroborate our findings. We show that somatic, but not axonal, K_V7/M-channels affect synaptic integration in a voltage-dependent manner in peri-somatic locations only. Axonal K_V7 channels, on the other hand, alter EPSP–spike coupling by lowering the action potential threshold. Modulation of EPSP–spike coupling may be another mechanism by which modification in K_V7/M-channel function may have a substantial impact on neuronal excitability and therefore, physiological processes such as learning and memory as well as patho-physiological conditions such as epilepsy (Jentsch, 2000; Peters *et al.* 2005; Wu *et al.* 2008).

Methods

Ethical approval

All experimental procedures were approved by the UK Home Office (Project licence PPL No. 70/06372) as well as the School of Pharmacy and UCL research ethics committees.

Electrophysiological studies

Methods used were similar to those described previously (see (Shah *et al.* 2008). Briefly, 5- to 6-week-old rats were anaesthetized and perfused intracardially with ice-cold modified ACSF containing (in mM): 110 choline chloride, 2.5 KCl, 1.25 NaH_2PO_4, 25 $NaHCO_3$, 0.5 $CaCl_2$, 7 $MgCl_2$ and 10 glucose, and bubbled continuously with 95% O_2–5% CO_2 to maintain pH at 7.2. Hippocampal–entorhinal slices, 400 μm thick, were prepared using a vibratome (Leica VT1000S). The slices were incubated in a holding chamber for 1 h at room temperature in external solution of the following composition (in mM): 125 NaCl, 2.5 KCl, 1.25 NaH_2PO_4, 25 $NaHCO_3$, 2 $CaCl_2$, 2 $MgCl_2$ and 10 glucose, and bubbled continuously with 95% O_2–5% CO_2 to maintain pH at 7.2. Whole-cell current-clamp recordings were obtained from both the soma and dendrites of CA1 pyramidal neurons. For recording purposes, slices were placed in a chamber containing external solution supplemented with 0.05 mM APV, 0.01 mM CNQX, 0.01 mM bicuculline and 0.001 mM CGP 55845 and maintained at 34–36°C. The internal pipette solution contained (in mM): 120 $KMeSO_4$, 20 KCl, 10 HEPES, 2 $MgCl_2$, 0.2 EGTA, 4 Na_2-ATP, 0.3 Tris-GTP and 14 Tris-phosphocreatine; pH was adjusted to 7.3 with KOH. Pipettes containing this internal solution had resistances of 8–9 MΩ. Whole-cell current-clamp recordings were obtained using a bridge-mode amplifier (Axoclamp 2A), filtered at 10 kHz and sampled at 30 kHz. Series resistances were usually of the order of 10–15 MΩ. Simulated EPSPs (αEPSPs) were generated by current injection of the order:

$$A = (t/\tau) * \exp(1 - (t/\tau))$$

where A is the amplitude of the current injected and τ is the rise time constant. All M-channel (KCNQ/Kv7) modulators were bath applied. All recordings were acquired using pCLAMP 8.0 and stored on a computer for further analysis.

Data analysis

All measurements were made using Clampfit (v8.0). The summation ratio was calculated as the amplitude of the fifth EPSP divided by the amplitude of the first. Group

data are expressed as mean $\pm$ SEM. Statistical significance was determined using either paired or unpaired Student's *t* tests as appropriate. Statistical significance of $P < 0.05$ is indicated as $*$ in all figures.

Materials

All chemicals were obtained from Sigma (St Louis, MO, USA) apart from XE991, CNQX, CGP 55845, bicuculline and APV, which were purchased from Tocris (USA). Retigabine was provided by NeuroSearch (Ballerup, Denmark) through EU grant LSHM-CT-2004-503038. ABP and sABP was custom made by Genscript (USA). Stock solutions of bicuculline and CGP 55845 were made in DMSO and stored at $-20°$C until use. These were then dissolved in the external solution such that the final DMSO concentration was less than 0.1%. Aqueous stock solutions of XE991, linopirdine, CNQX and APV were also kept at $-20°$C until use.

Computational modelling methods

All simulations were implemented and run with the NEURON program (v7.1) (Hines & Carnevale, 1997) using the variable time step feature. The 3D reconstruction of the CA1 pyramidal neuron was one of those used in a previous work (neuron 9068802, Migliore *et al.* 2005). The same standard, uniform, passive properties were used for control conditions ($\tau_m = 28$ ms, $R_m = 28$ kΩ cm^2, $R_a = 150$ Ω cm). Resting potential was set at -65 mV and at 35°C. All channel kinetic and distribution were from a previously published model (Shah *et al.* 2008), and based on the available experimental data for CA1 pyramidal neurons (reviewed in Migliore & Shepherd, 2002). Sodium and delayed rectifier potassium conductances were uniformly distributed throughout the dendrites, whereas an A-type potassium and a non-specific I_h conductance were linearly increasing with distance from the soma. The K_V7-type potassium conductance was inserted into the soma and at a 3-fold higher density in the axon (Shah *et al.* 2008). To take into account for Ca^{2+} channels open around resting potential (reviewed in Marder & Goaillard, 2006), a low-threshold Ca^{2+} and Ca^{2+}-dependent K^+ conductances together with a simple Ca^{2+} extrusion mechanism were included at uniform density and distribution in all compartments. The simulation files are available for public download under the ModelDB section (Migliore *et al.* 2003) of the Senselab database (http://senselab.med.yale.edu). The effects of XE991 application were modelled by deleting the K_V7/M-conductance.

Results

To determine if Kv7 (M-) channels affect post-synaptic EPSP kinetics and summation at the soma and dendrites,

individual EPSPs as well as 20 and 40 Hz trains of EPSPs were induced post-synaptically by injecting an alpha waveform current (Poolos *et al.* 2002; Shah *et al.* 2004) (see Methods) into either the soma or dendrite. These somatic and dendritic αEPSPs had similar kinetics to those evoked by stimulating the Schaffer collaterals in the stratum radiatum. We chose this method to avoid complications due to possible pre-synaptic effects of K_V7 channels (Martire *et al.* 2004; Peretz *et al.* 2007; Luisi *et al.* 2009; Huang & Trussell, 2011). Experiments were done in the presence of 1 μM TTX to prevent spontaneous action potential firing in the presence of the K_V7/M-channel inhibitor, XE991 (Shah *et al.* 2008). At -60 mV, 3 μM XE991 enhanced the amplitude of somatic αEPSPs by $34.7 \pm 11\%$ ($n = 6$, $P < 0.05$, Fig. 1*A*) and lengthened the decay time constant (τ) by $92.3 \pm 28\%$ ($n = 6$, $P < 0.05$, Fig. 1*A*). Consistent with the M-current biophysical properties in these neurons (Shah *et al.* 2008), the actions of XE991 were voltage dependent with significantly smaller effects at -70 mV (% change in amplitude and τ were $23.2 \pm 3.1\%$ ($n = 6$) and $28.7 \pm 7.4\%$ ($n = 6$, $P < 0.05$), respectively, Fig. 1*A*). The K_V7/M-channel enhancer, retigabine (10 μM), on the other hand, had little effect on somatic αEPSP amplitudes at either -70 mV or -60 mV (Fig. 1*B*). It significantly reduced τ at -60 mV by $41.8 \pm 3.8\%$ ($n = 9$, $P < 0.05$) but not at -70 mV (Fig. 1*B*). Neither retigabine nor XE991 had any effect on dendritic αEPSPs (Fig. 1*A* and *B*), as would be expected for a significantly lower dendritic K_V7 channel density (Yue & Yaari, 2006; Hu *et al.* 2007; Shah *et al.* 2008).

Since the K_V7 modulators affected somatic αEPSP decay time constants at -60 mV, it is likely that they may also modulate αEPSP integration at that voltage. Indeed, at -60 mV XE991 and retigabine significantly enhanced and reduced, respectively, the summation of 20 Hz and 40 Hz trains of somatic 5 αEPSPs (Fig. 2*A* and *B*). Removal of TTX, in the presence of XE991, resulted in spikes during the somatic αEPSP train irrespective of the frequency, indicating that EPSP–spike coupling had increased (data not shown).

Interestingly, retigabine, unlike XE991 (Fig. 2*A*), affected somatic αEPSP summation at -70 mV (Fig. 2*B*). The effects were less than that at -60 mV (Fig. 2*B*), consistent with the much reduced effect of the compound on the decay time constants of single αEPSPs (Fig. 1*B*). Retigabine shifts the activation curve of K_V7/M-current to the left in neurons (Tatulian *et al.* 2001; Shah *et al.* 2008). Hence, in the presence of retigabine, channel opening occurs at lower voltages and so summation is likely to be more affected by retigabine at -70 mV than by XE991.

Neither XE911 nor retigabine altered dendritic αEPSP summation (Fig. 2*A* and *B*), in agreement with the lack of effects of the compounds on single dendritic αEPSPs and the notion that fewer K_V7 channels are located in

dendrites (Yue & Yaari, 2006; Hu *et al.* 2007; Shah *et al.* 2008).

To verify the interpretation of the above results, we performed computer simulations using a model that we had previously found best mimicked the changes in firing patterns of CA1 neurons following K_V7 channel

inhibition (see Shah *et al.* 2008). Na^+ channels were not included in these simulations as in our experimental conditions Na^+ channels had been inhibited by TTX. Compatible with the experimental results, K_V7 channel deletion throughout the neuron enhanced 20 Hz (Fig. 3*A*) and 40 Hz EPSP summation at the soma at -60 mV.
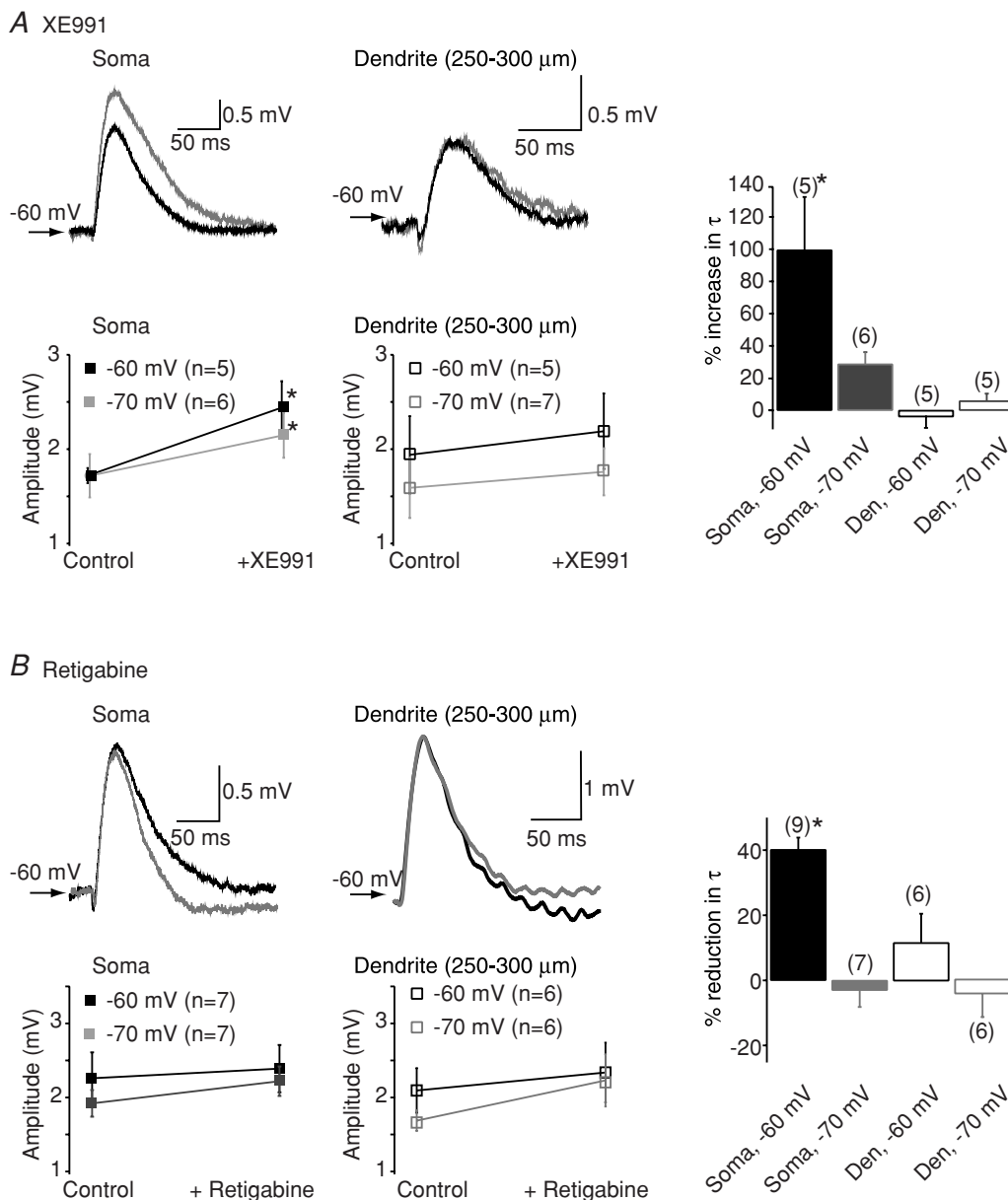

Figure 1. Example traces showing the effects of (*A*) the K_V7/M-channel blocker XE991 (3 μM) and (*B*) the K_V7/M-channel enhancer retigabine (10 μM) on simulated EPSP (αEPSP) shapes at the soma and dendrites when evoked at a potential of -60 mV

Black traces represent controls whereas the grey traces are those obtained following bath application of the K_V7/M-channel modulator. Shown below the traces are the average (mean and SEM) somatic and dendritic αEPSP amplitudes in the absence and presence of (*A*) XE991 and (*B*) retigabine at potentials of -60 mV and -70 mV. The observations for each point are indicated in brackets next to the potential. Within each panel, the percentage change in the decay time constant (τ) of αEPSPs at the soma and dendrites at either -60 mV or -70 mV is illustrated in the graph on the far right. In these particular graphs, the numbers of observations are indicated above each bar. *Significance at $P < 0.05$.

The increase in summation was less than at -70 mV (Fig. 3*A*), consistent with the biophysical properties of K$_V$7 channels in hippocampal pyramidal cells (Shah *et al.* 2008). Dendritic EPSP summation, though, was not affected at either frequency at -60 mV or -70 mV (Fig. 3*B* for example traces at 20 Hz). These findings support the idea that K$_V$7 channels are principally located at the soma/axon and affect peri-somatic post-synaptic EPSP integration.

We next asked whether axonal or somatic K$_V$7 channels differentially affect EPSP integration. In computer simulations, removal of axonal K$_V$7 channels but leaving somatic channels intact, had little impact on EPSP summation at the soma (Fig. 3*C*). In contrast, elimination of somatic K$_V$7 channels with axonal K$_V$7 channels

still present significantly enhanced summation (Fig. 3*C*). These results indicate that only somatic K$_V$7 channels affect peri-somatic EPSP summation.

To test if this is so experimentally, we used a competing peptide, ABP (YIAEGESDTD), that is designed to selectively disrupt the coupling of K$_V$7 channels to ankyrin G, and thereby alter K$_V$7 channel function in the axon (see Shah *et al.* 2008). Hence, unlike XE991 or retigabine, bath application of which would affect all channels within the neuron, this peptide only affects axonal K$_V$7 channels. Indeed, we have previously shown that the peptide had little effect on somatic M-current measured with voltage clamp (Shah *et al.* 2008). Inclusion of this peptide (10 mM) in the intracellular pipette solution caused RMP depolarization from -68 ± 0.7 mV
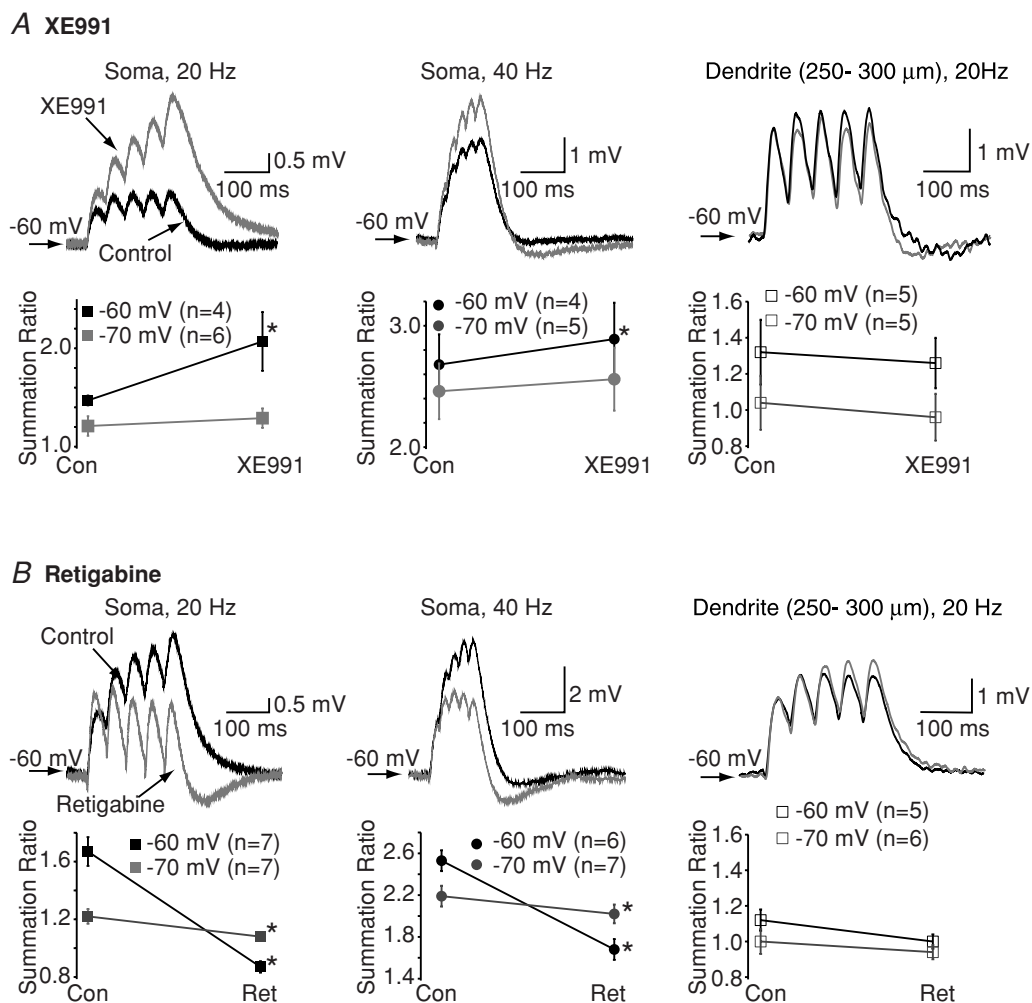

Figure 2. Representative illustrations showing trains of 20 Hz or 40 Hz somatic and dendritic αEPSPs in the absence (black) and presence (grey) of either (*A*) 3 μM XE991 or (*B*) 10 μM retigabine at a potential of -60 mV
The summation ratio was calculated as the amplitude of the fifth αEPSP divided by the amplitude of the first αEPSP (see Methods). Below each of the examples are graphs showing the mean and SEM of the summation ratio for the particular frequency at potentials of either -60 mV or -70 mV. The numbers of observations for each frequency at a particular potential are indicated in parentheses within each graph. *Significance at $P < 0.05$.

to -60.9 ± 1.4 mV ($n = 8$, $P < 0.05$) within 25 min (Fig. 4A). The action potential threshold was also lowered by 4.9 ± 1.3 mV ($n = 7$, $P < 0.05$, Fig. 4A) as described previously (Shah *et al.* 2008). As a consequence, the action potential firing rate increased substantially, with 5 out of 8 neurons firing spontaneously as reported previously (Shah *et al.* 2008). However, unlike XE991 (Hu *et al.* 2007; Shah *et al.* 2008), the somatic input resistance as measured using a 400 ms, 50 pA depolarizing step from a fixed potential of -70 mV was unaffected by ABP (% change $= -2.9 \pm 22.6\%$, $n = 7$). Inclusion of a scrambled ABP (TSEYDAEDIG, 10 mM) had little effect on resting membrane potential (Fig. 4B), action potential firing (Fig. 4B), action potential threshold (Fig. 4B) or input resistance (% change $= 13.9 \pm 21.8\%$, $n = 3$) over a period of 45–60 min.

We then tested the effects of ABP on single and trains of αEPSPs generated at the soma. In contrast to XE991 (Fig. 1A), in the presence of TTX, single αEPSPs were unaffected by ABP at -60 mV (% increase in amplitude and $\tau = 4.3 \pm 12.0\%$ ($n = 4$) and $-6.5 \pm 10.7\%$ ($n = 4$), respectively). Thus, not surprisingly, trains of 20 Hz and 40 Hz αEPSPs were unaffected by 30 min ABP treatment at -60 mV (Fig. 5A). Removal of TTX resulted in action potentials being elicited in 60% (3/5) of neurons with 40 Hz αEPSP trains and in 50% (2/4) of neurons with 20 Hz αEPSP trains (Fig. 5A), presumably because ABP lowers the action potential threshold (Fig. 4A). Inclusion of scrambled ABP (sABP) in the pipette solution for 45 min had no effect on single (% increase in amplitude and $\tau = 9.2 \pm 12.3\%$ ($n = 6$, $P = 0.7$) and $9.0 \pm 14.7\%$ ($n = 6$, $P = 0.4$), respectively) or trains of αEPSPs ($n = 6$, Fig. 5). Further, washing out TTX did not result in spikes with αEPSP trains if sABP was included in the patch pipette. Hence, disruption of axonal or somatic K_V7 channel function is likely to alter EPSP–spike

A Somatic simulated EPSPs in the absence and presence of all K_V7 channels
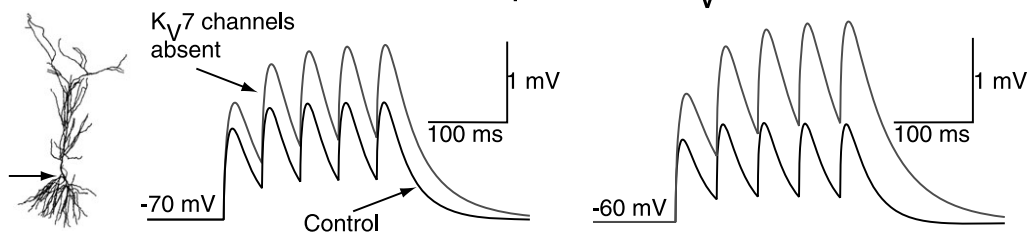
B Dendritic simulated EPSPs with and without all K_V7 channels
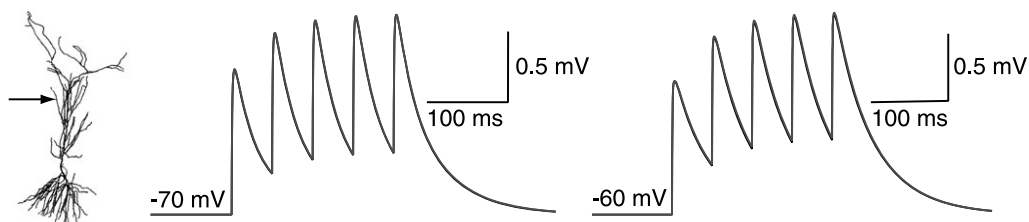
C Removing axonal or somatic K_V7 channel density in a CA1 pyramidal cell model
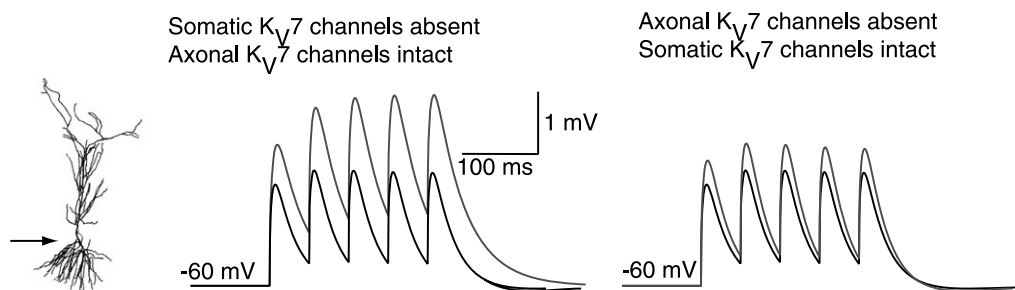

Figure 3. Twenty hertz trains of EPSPs obtained using computer simulations with (black) and without (red) K_V7/M-channels at the soma (A) and dendrites (B)
The simulations were obtained at -70 mV and -60 mV. C, computer simulations showing 20 Hz αEPSP traces under control (black) conditions and following the selective removal of either somatic or axonal K_V7/M-channel density (grey). The simulations were performed at -60 mV. The scale bar shown applies to both traces.

coupling. However, only somatic K$_V$7 channels affect EPSP integration at the soma.

Discussion

Post-synaptic K$_V$7/M-channels have been shown to modulate action potential firing in a number of

different cell types (pyramidal neurons as well as interneurons; Brown & Passmore, 2009). Here, we show that post-synaptic K$_V$7 channels also affect synaptic integration in a location-dependent manner in CA1 pyramids. Bath application of K$_V$7 channel modulators affected somatic but not dendritic synaptic potential shapes (Fig. 1) and summation (Fig. 2) in a voltage-dependent manner, in agreement with the reported biophysical properties of
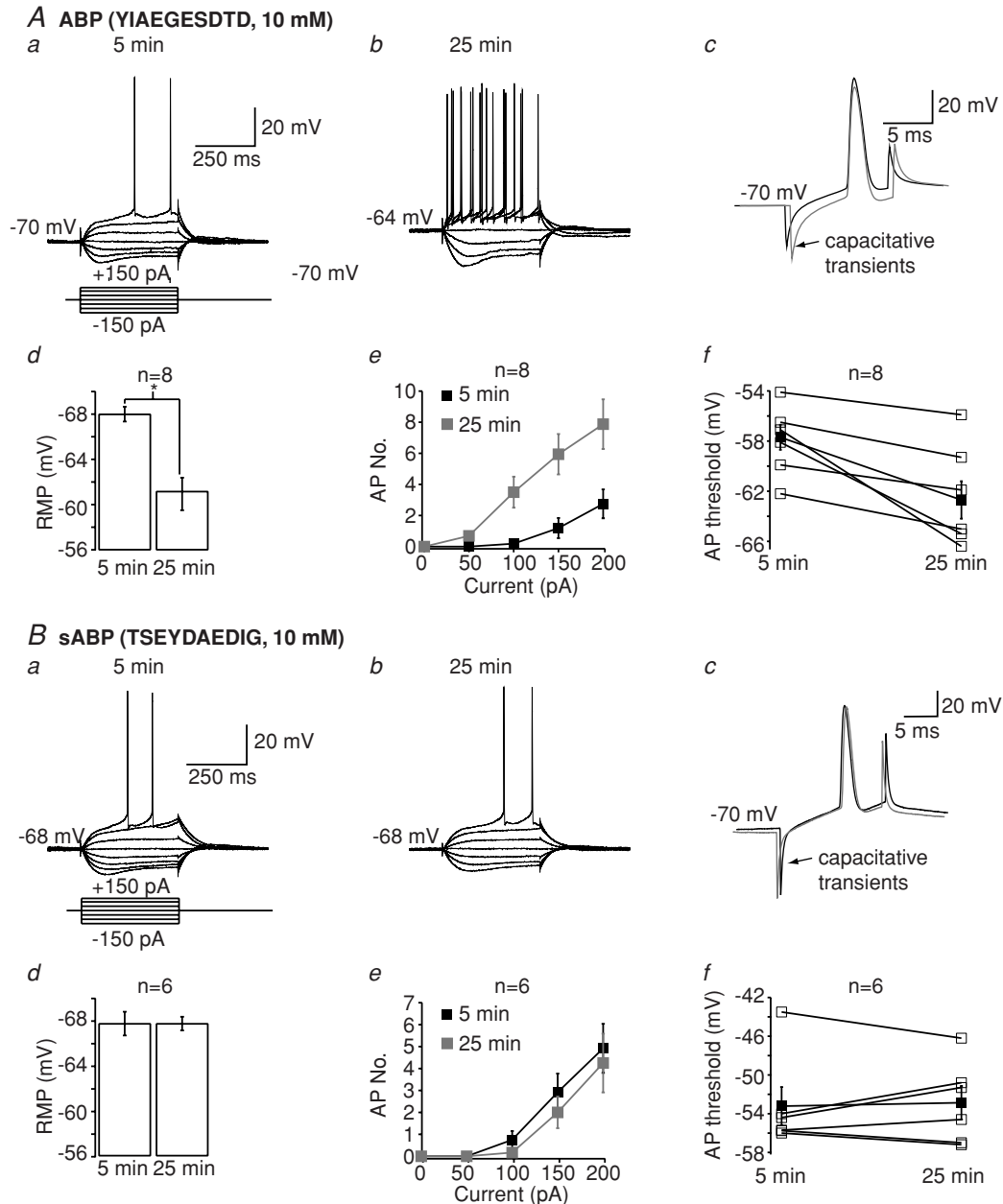

Figure 4. Effects of ABP and sABP on action potential firing and resting membrane potential
Aa, *Ba*, *Ab* and *Bb*, examples of traces 5 min and 25 min after obtaining whole-cell patch clamp when ABP (*A*) or sABP (*B*) is included in the patch pipette solution. *Ac* and *Bc*, representative traces showing the influence of ABP and sABP on action potential threshold 5 min (black) and 25 min (grey) after breakthrough. The alterations in resting membrane potential, the number of action potentials and the action potential threshold when either ABP or sABP are present in the patch pipette are shown in *Ad*, *Bd*, *Ae*, *Be*, *Af* and *Bf*. In panels *Af* and *Bf*, the filled squares represent the mean and standard error whereas the open squares show the individual responses.

the M-current in hippocampal CA1 pyramids (Shah *et al.* 2008). These results were reproducible by computer modelling (Fig. 3). Hence, K_V7/M-channels are likely to be primarily located in the peri-somatic region (Yue & Yaari, 2006; Hu *et al.* 2007; Shah *et al.* 2008).

In our experiments, most synaptic transmission was blocked. K_V7/M-channels may be present on pre-synaptic terminals in the hippocampus (Martire *et al.* 2004; Peretz *et al.* 2007). Therefore, though post-synaptic K_V7/M-channels do not affect dendritic synaptic potentials directly, modulation of synaptic release by pre-synaptic K_V7/M-channels may additionally affect dendritic excitability and synaptic integration.

K_V7/M-channels are likely to be present predominantly in the axon initial segment (Devaux *et al.* 2004; Chung *et al.* 2006; Pan *et al.* 2006; Shah *et al.* 2008). However, our data suggested that only somatic channels altered somatic synaptic potential shapes and summation as bath application of XE991 and retigabine (which would affect all K_V7 channels in a neuron) modified somatic EPSP summation (Fig. 2) whereas use of the competing peptide, ABP, had little effect (Fig. 5). In these neurons, ABP modulates only axonal K_V7 channels as it lowered the

action potential threshold without changing the input resistance (Fig. 4 and Results). In contrast, treatment with XE991, which would inhibit all K_V7 channels, reduced the action potential threshold and increased the input resistance (see Shah *et al.* 2008). Further, we have previously shown that bath application of XE991 after ABP has had its full effect causes little further decrease in action potential threshold (Shah *et al.* 2008). These data thus suggest that ABP affects axonal K_V7 channels only. In addition, the notion that somatic but not axonal K_V7 channels affected summation was supported by data obtained using computer simulations (Fig. 3*C*). Since somatic K_V7 channels influence somatic input resistance (Shah *et al.* 2008), and variations in input resistance lead to changes in synaptic potential shapes (Magee, 2000), this may explain why only K_V7 channels located at the cell body modified synaptic integration. These results therefore suggest that the effects of K_V7 channels on synaptic integration are locally mediated. Since recent evidence suggests synaptic potentials can propagate along axons (Clark & Hausser, 2006), we cannot exclude the possibility that axonal K_V7 channels may influence shapes and summation of synaptic potentials within these structures.
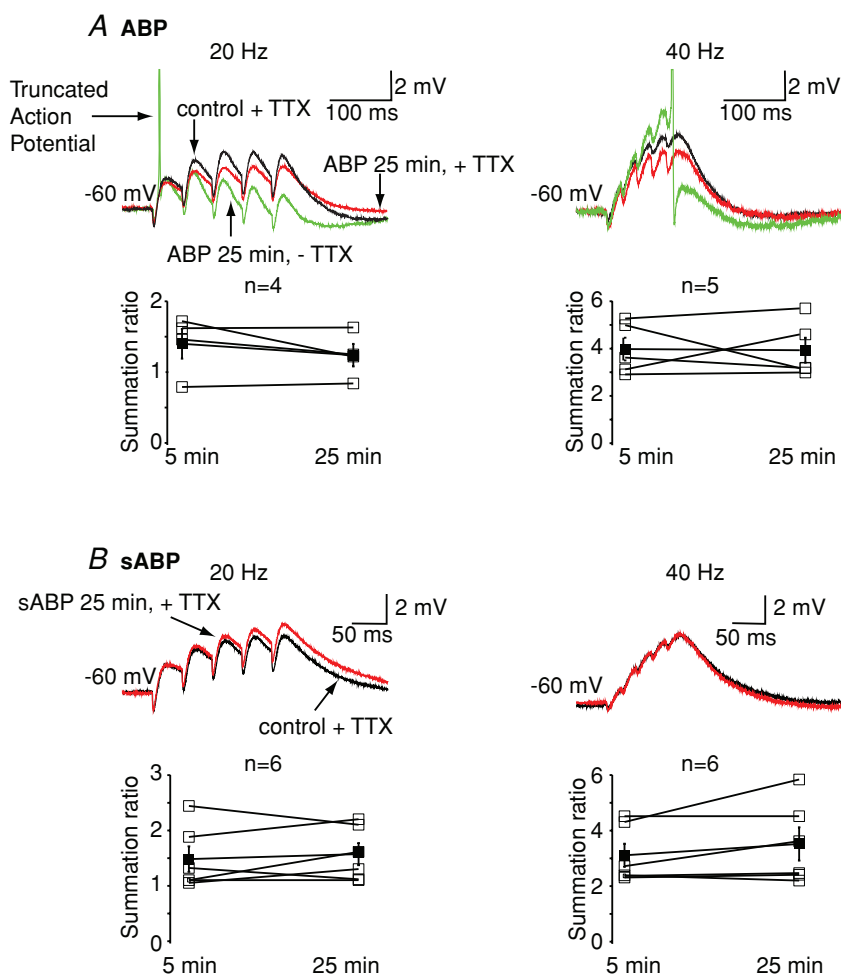

Figure 5. Axonal K_V7 channels have little effect on somatic αEPSP summation

A, example traces showing the effects of including the ankyrin G binding peptide (ABP, 10 mM) in the intracellular pipette solution on 20 Hz and 40 Hz trains of αEPSPs. The traces within 5 min of going whole cell are deemed control (see (Shah *et al.* 2008) and are in black. The maximal effect of ABP occurs within 25 min (Shah *et al.* 2008) and is shown in red. TTX was present throughout. Washout of TTX resulted in spikes (AP; green trace). Generation of spikes will cause an afterdepolarization and/or afterhyperpolarization, which will affect αEPSP summation. Indeed, in the particular example shown, the action potential resulted in an afterdepolarization followed by an afterhyperpolarization, thereby distorting the αEPSP summation. For this reason, αEPSP summation ratios were calculated from traces in the which TTX was present in the external solution. The average (mean and SEM; filled squares) and individual (open squares) calculated summation ratios following 5 min and 25 min of patching with pipettes containing ABP in the presence of external TTX are shown below the traces. *B*, representative traces showing the effects of scrambled ABP (sABP, 10 mM) on 20 Hz and 40 Hz trains of αEPSPs within 5 min of going whole cell (control, black) or after 25 min (red). All experiments were performed in the presence of TTX. The individual (open squares) and mean (filled squares) calculated summation ratios for all cells in which sABP was included in the pipette are shown below.

Indeed, recent evidence shows that K_V7 channels located in immature synaptic terminals alter inhibitory depolarizing synaptic potential shapes and integration in the bouton, suggesting that K_V7 channels exert a local effect on synaptic integration within a particular neuronal sub-cellular compartment (Huang & Trussell, 2011).

By modulating spike threshold and the resting membrane potential of neurons (Fig. 4; Shah *et al.* 2008), axonal K_V7 channels can affect global cell excitability too. Thus, though ABP did not affect somatic synaptic integration *per se*, EPSP–spike coupling was enhanced as the action potential threshold was reduced (Fig. 5). This also raises the possibility that the manner in which K_V7 channels affect cell excitability may depend on the cellular compartment in which they are expressed. Since these channels are modulated by a variety of neurotransmitters and intracellular signalling molecules (Delmas & Brown, 2005), this may provide an exquisite mechanism by which K_V7 channels can fine-tune a cell's intrinsic activity in response to changing neural network excitability and thereby influence physiological processes such as plasticity and learning as well as prevent neurological disorders such as epilepsy (Jentsch, 2000; Peters *et al.* 2005; Wu *et al.* 2008).

References

Brown DA & Passmore GM (2009). Neural KCNQ (Kv7) channels. *Br J Pharmacol* **156**, 1185–1195.

Chung HJ, Jan YN & Jan LY (2006). Polarized axonal surface expression of neuronal KCNQ channels is mediated by multiple signals in the KCNQ2 and KCNQ3 C-terminal domains. *Proc Natl Acad Sci U S A* **103**, 8870–8875.

Clark B & Hausser M (2006). Neural coding: hybrid analog and digital signalling in axons. *Curr Biol* **16**, R585–R588.

Debanne D (2004). Information processing in the axon. *Nat Rev* **5**, 304–316.

Delmas P & Brown DA (2005). Pathways modulating neural KCNQ/M (Kv7) potassium channels. *Nat Rev* **6**, 850–862.

Devaux JJ, Kleopa KA, Cooper EC & Scherer SS (2004). KCNQ2 is a nodal K^+ channel. *J Neurosci* **24**, 1236–1244.

Goldman AM, Glasscock E, Yoo J, Chen TT, Klassen TL & Noebels JL (2009). Arrhythmia in heart and brain: KCNQ1 mutations link epilepsy and sudden unexplained death. *Sci Transl Med* **1**, 2ra6.

Hines ML & Carnevale NT (1997). The NEURON simulation environment. *Neural Comput* **9**, 1179–1209.

Hu H, Vervaeke K & Storm JF (2007). M-channels (Kv7/KCNQ channels) that regulate synaptic integration, excitability, and spike pattern of CA1 pyramidal cells are located in the perisomatic region. *J Neurosci* **27**, 1853–1867.

Huang H & Trussell LO (2011). KCNQ5 channels control resting properties and release probability of a synapse. *Nat Neurosci* **14**, 840–847.

Jentsch TJ (2000). Neuronal KCNQ potassium channels: physiology and role in disease. *Nat Rev* **1**, 21–30.

Luisi R, Panza E, Barrese V, Iannotti FA, Viggiano D, Secondo A, Canzoniero LM, Martire M, Annunziato L & Taglialatela M (2009). Activation of pre-synaptic M-type K^+ channels inhibits [^{3}H]D-aspartate release by reducing Ca^{2+} entry through P/Q-type voltage-gated Ca^{2+} channels. *J Neurochem* **109**, 168–181.

Magee JC (2000). Dendritic integration of excitatory synaptic input. *Nat Rev* **1**, 181–190.

Marder E & Goaillard JM (2006). Variability, compensation and homeostasis in neuron and network function. *Nat Rev* **7**, 563–574.

Martire M, Castaldo P, D'Amico M, Preziosi P, Annunziato L & Taglialatela M (2004). M channels containing KCNQ2 subunits modulate norepinephrine, aspartate, and GABA release from hippocampal nerve terminals. *J Neurosci* **24**, 592–597.

Migliore M, Ferrante M & Ascoli GA (2005). Signal propagation in oblique dendrites of CA1 pyramidal cells. *J Neurophysiol* **94**, 4145–4155.

Migliore M, Morse TM, Davison AP, Marenco L, Shepherd GM & Hines ML (2003). ModelDB: making models publicly accessible to support computational neuroscience. *Neuroinformatics* **1**, 135–139.

Migliore M & Shepherd GM (2002). Emerging rules for the distributions of active dendritic conductances. *Nat Rev Neurosci* **3**, 362–370.

Pan Z, Kao T, Horvath Z, Lemos J, Sul JY, Cranstoun SD, Bennett V, Scherer SS & Cooper EC (2006). A common ankyrin-G-based mechanism retains KCNQ and NaV channels at electrically active domains of the axon. *J Neurosci* **26**, 2599–2613.

Peretz A, Sheinin A, Yue C, Degani-Katzav N, Gibor G, Nachman R, Gopin A, Tam E, Shabat D, Yaari Y & Attali B (2007). Pre- and postsynaptic activation of M-channels by a novel opener dampens neuronal firing and transmitter release. *J Neurophysiol* **97**, 283–295.

Peters HC, Hu H, Pongs O, Storm JF & Isbrandt D (2005). Conditional transgenic suppression of M channels in mouse brain reveals functions in neuronal excitability, resonance and behavior. *Nat Neurosci* **8**, 51–60.

Poolos NP, Migliore M & Johnston D (2002). Pharmacological upregulation of h-channels reduces the excitability of pyramidal neuron dendrites. *Nat Neurosci* **5**, 767–774.

Roche JP, Westenbroek R, Sorom AJ, Hille B, Mackie K & Shapiro MS (2002). Antibodies and a cysteine-modifying reagent show correspondence of M current in neurons to KCNQ2 and KCNQ3 K^+ channels. *Br J Pharmacol* **137**, 1173–1186.

Shah MM, Anderson AE, Leung V, Lin X & Johnston D (2004). Seizure-induced plasticity of h channels in entorhinal cortical layer III pyramidal neurons. *Neuron* **44**, 495–508.

Shah MM, Migliore M, Valencia I, Cooper EC & Brown DA (2008). Functional significance of axonal Kv7 channels in hippocampal pyramidal neurons. *Proc Natl Acad Sci U S A* **105**, 7869–7874.

Shah MM, Mistry M, Marsh SJ, Brown DA & Delmas P (2002). Molecular correlates of the M-current in cultured rat hippocampal neurons. *J Physiol* **544**, 29–37.

Tatulian L, Delmas P, Abogadie FC & Brown DA (2001). Activation of expressed KCNQ potassium currents and native neuronal M-type potassium currents by the anti-convulsant drug retigabine. *J Neurosci* **21**, 5535–5545.

Wu WW, Chan CS, Surmeier DJ & Disterhoft JF (2008). Coupling of L-type Ca^{2+} channels to KV7/KCNQ channels creates a novel, activity-dependent, homeostatic intrinsic plasticity. *J Neurophysiol* **100**, 1897–1908.

Yue C & Yaari Y (2006). Axo-somatic and apical dendritic Kv7/M channels differentially regulate the intrinsic excitability of adult rat CA1 pyramidal cells. *J Neurophysiol* **95**, 3480–3495.

Author contributions

M.M.S. and D.A.B. designed experiments. M.M.S. performed and analysed all experiments. M.M. performed computer simulations. M.M.S. and D.A.B. wrote the manuscript. All authors approved the final version.

Acknowledgements